Journal of
Materials Chemistry B

Materials for biology and medicine

Accepted Manuscript

This article can be cited before page numbers have been issued, to do this please use: A. Raza, P. Reginold, N. Skalko-Basnet and S. A. O. Obuobi, *J. Mater. Chem. B*, 2026, DOI: 10.1039/D5TB02868J.

ROYAL SOCIETY OF CHEMISTRY

rsc.li/materials-b

View Article Online
DOI: 10.1039/D5TB02868J

ARTICLE

Polyethylene oxide-poloxamer 407 *in situ* forming gels: A dual-drug delivery system for periodontal application

Received 00th January 20xx,
Accepted 00th January 20xx

DOI: 10.1039/x0xx00000x

Ali Raza, Piarina Reginold, Nataša Škalko-Basnet, Sybil Obuobi*

Periodontitis is an infectious and inflammatory disease that requires prolonged localized antibacterial and anti-inflammatory treatment. *In situ* forming gel (ISFG) drug delivery systems offer a promising approach for localized periodontal drug delivery. Poloxamer 407 (P407) is a well-reported thermosensitive polymer for ISFG systems; however, its low mechanical strength limits its ability to withstand *in vivo* stress. Herein, we utilized polyethylene oxide (PEO) to increase the mechanical strength of poloxamer 407 (P407)-based *in situ* gels, particularly for periodontal delivery of antibacterial (metronidazole) and antioxidant/anti-inflammatory drugs (curcumin). First, two types of formulations were developed: one containing the hydrophilic drug metronidazole (MTD) and the other with hydrphobic curcumin-loaded zein nanoparticles (CZ) to evaluate the effect of PEO. The prepared systems were assessed for gelation time, gelation temperature, syringeability, gel hardness, adhesiveness, drug release, and degradation. The addition of PEO significantly enhanced gel hardness and adhesiveness, and the syringeability force (but within a reported acceptable limit of 40 N); however, PEO did not affect the release of MTD. The cytocompatibility of the formulations was not compromised by presence of PEO. CZ-loaded gels also exhibited antioxidant and anti-inflammatory activities via DPPH scavenging assay and in LPS-polarized macrophages, respectively. The P407 system with curcumin nanoparticles showed a significant increase in syringeability force during storage, whereas the PEO-P407 system maintained stable syringeability over 2 months. Lastly, both drugs were incoporated into a single formulation with PEO, and their release profiles were comparable to those observed in formulations containing the individual drugs. This indicates that the combined formulation did not adversely affect the release of either drugs nor influence the antibacterial activity. In conclusion, these findings indicate that PEO can improve both the mechanical properties and stability of nanoparticles-loaded P407-based gels with the ability to deliver hydrophilic and hydrophobic drug-loaded nanoparticles.

1. Introduction

Periodontitis is a prevalent chronic inflammatory disease involving the damage of periodontal tissues (including the gingiva, periodontal ligament, and alveolar bone), primarily caused by bacterial infection and host immune response.[1] Anaerobic bacteria such as *Porphyromonas gingivalis*, *Aggregatibacter actinomycetemcomitans*, and *Tannerella forsythia* are predominantly involved in causing periodontal infection.[2] Conventional treatments include mechanical debridement (scaling and root planing), systemic or local antibiotic administration, and surgical interventions to control infection and inflammation.[3] However, these approaches have limitations, such as the need for repeated procedures, poor drug retention at the target site, and systemic side effects.[4] Thus, prolonged localized antibiotic treatment is desirable for treating periodontitis to avoid repeated procedures and systemic side effects.

For localized treatment, *in situ* forming implants (ISFI) and *in situ* forming gel drug delivery systems (ISFG-DDS) have gained significant attention. These systems undergo sol-to-implant or sol-to-gel transition under physiological conditions, thus facilitating easy administration and prolonged residence time.[5-7] . Most of the reported ISFI systems are based on the solvent removal precipitation principle, in which organic solvents permeate into the surrounding body fluid, causing the formation of a polymeric insoluble implant.[8, 9] Although it is a promising approach, organic solvents may induce toxic effects and challenges in regulatory approval. On the other hand, ISFG-DDS can form gel upon injection and are biocompatible due to the high concentration of water.[10] Consequently, ISFG-DDS are preferred, but their inherent low mechanical strength is a barrier to their success.[10]

Poloxamer 407 (P407), a thermosensitive triblock copolymer (PEO-PPO-PEO), is a widely used polymer in ISFG-DDS due to its thermosensitive gelation at physiological temperatures.[11-13] P407 solution can easily be injected into the periodontal pocket due to its low viscosity. Upon exposure to body temperature, it undergoes rapid gelation, forming a gel that enables prolonged site retention with sustained drug release.[14] Despite its advantage of thermosensitive gelling, P407-based gels suffer from several drawbacks, such as weak mechanical properties [15] and the need for organic cosolvents to incorporate hydrophobic drugs.[16] Considering the drugs for periodontitis treatment,

Drug Transport and Delivery Research Group, The Department of Pharmacy, UiT The Arctic University of Norway, Universitetsveien 57, 9037 Tromsø, Norway
**Corresponding author; sybil.obuobi@uit.no*

View Article Online
DOI: 10.1039/D5TB02681

metronidazole (MTD), a hydrophilic nitroimidazole antibiotic, is commonly used for periodontitis treatment due to its efficacy against anaerobic bacteria.[17] However, modulating the host inflammatory response and alleviating oxidative stress are also essential in controlling periodontal tissue destruction.[18] Curcumin, a hydrophobic phytochemical, exhibits antibacterial activity against periodontal pathogens and potent anti-inflammatory effects by inhibiting NF-κB and cytokine production.[19] Combining MTD and curcumin in a single delivery system could provide synergistic benefits by simultaneously targeting bacterial infection, inflammation, and oxidative stress.[20, 21] However, formulating a dual-drug delivery system with both hydrophilic and hydrophobic drugs is challenging due to their different solubility profiles. MTD can be directly dissolved in P407 solutions, while curcumin requires encapsulation in nano-carriers to enhance its dispersibility and stability. Optimizing the P407 gel matrix to accommodate both drug types without compromising syringeability or stability is essential.

To address the mechanical weakness of P407 gels, polymeric additives, such as chitosan,[22] gellan gum,[23] poly(acrylic Acid),[24] and alginate[25] have been explored. However, their addition can affect syringeability[22, 26] and the complex ionic nature of these polymers may cause aggregation of nanocarriers. Polyethylene oxide (PEO) may enhance hydrogel viscosity, mechanical strength, and mucoadhesion due to its entanglement with P407 micelles[27, 28] and may also minimally interact with loaded nanoparticles due to its nonionic nature. The mechanical reinforcement of P407 gels using PEO and its effect on encapsulated nanoparticles' stability and injectability have not been explored to our knowledge. Moreover, most of the studies reported for P407-based ISGF-DDS for periodontal applications were based on a single type of drug delivery (either hydrophilic or hydrophobic), overlooking the potential benefits of dual-drug systems.

This study has two primary objectives. The first is to enhance the mechanical strength of P407 ISFG by incorporating PEO as an additive and to evaluate the effect of PEO on the properties of ISFG for both hydrophilic and hydrophobic drug delivery. The second objective is to develop a dual-drug-loaded (MTD and curcumin-zein nanoparticles) P407-PEO ISFG for periodontitis, leveraging the combined antibacterial activity of MTD and the anti-inflammatory and antioxidant activities of curcumin. The effect of PEO on gel strength, syringeability force, and drug release was evaluated. The cytocompatibility against human dermal fibroblasts (HDF) and antibacterial efficacy against *P. gingivalis* were assessed. The stability study at 4 °C was assessed for 2 months to provide proof-of-concept that PEO is not a destabilizing factor for the ISFG. This study demonstrates PEO's role in enhancing the mechanical strength and stability of P407-based ISFG, which offers a simple approach for the delivery of hydrophilic and hydrophobic drugs in periodontitis therapy.

2. Materials and Methods

2.1. Materials

L-ascorbic acid, 2,2-diphenyl-1-picrylhydrazyl (DPPH), ethanol 96%, fetal bovine serum (FBS), sodium phosphate dibasic dihydrate, sodium chloride, and poloxamer 407 were obtained from Sigma-Aldrich (Steinheim, Germany); Brain Heart Infusion Broth (BHI), potassium phosphate monobasic, and trypsin-EDTA solution were purchased from Sigma-Aldrich (St. Louis, USA); curcumin and metronidazole were from Fluka; dimethyl sulfoxide (DMSO) was from MP Biomedicals (Solon, USA); DMEM high glucose was from Biowest; fluorescein diacetate (FDA) was from Thermo Scientific (UK); thiazolyl blue tetrazolium bromide (MTT) was from Thermo Scientific (Kandel, Germany); glycerol 86% was from VWR Chemicals (Leuven, Belgium); phosphate-buffered saline (PBS) was from Gibco (Paisley, UK); polyethylene oxide (PEO, MW 900,000 g/mol) was from Dow Chemical Company (Midland, MI, USA); and zein was from Tokyo Chemical Industry (Toshima, Kita-Ku, Tokyo, Japan).

2.2. Preparation of curcumin-loaded zein nanoparticles (CZNP)

Curcumin-loaded zein nanoparticles (CZ) were prepared using the nanoprecipitation method.[29, 30] Curcumin (1 mg/mL) was prepared in 70% v/v ethanol (in water). Different amounts of zein (50, 75, or 100 mg) were added to this solution (2 mL) and dissolved using a spatula. After 1 h of equilibration, 2 mL of the resulting solution was added dropwise into 6 mL of an aqueous solution containing 1 % P407 (w/v, in water) (acting as a stabilizer) under continuous magnetic stirring (800 rpm) and allowed to stir for 1.5 h at room temperature in the fume hood to evaporate ethanol that was verified by weight change. The entire process was conducted in the dark (using aluminum foil to cover the sides of the beaker) to prevent curcumin degradation. These nanoparticles were named CZ50, CZ75, and CZ100 based on the corresponding zein concentration used, i.e., 50, 75, and 100 mg, respectively. Zein nanoparticles without curcumin were also prepared for cell studies, named Z50, corresponding to 50 mg of zein.

2.3. Characterization of Nanoparticles

2.3.1. Particle Size and Zeta Potential Analysis

The hydrodynamic diameter (size), polydispersity index (PDI), and zeta potential of the NPs were determined using dynamic light scattering (DLS) (ZetaSizer Nano ZS, Malvern Instruments). Before analysis, the samples were diluted (10 µL of NPs in 990 µL distilled water). Measurements were performed in triplicate at 25 °C, with each run consisting of three cycles.

2.3.2. Determination of Entrapment Efficiency (EE)

The entrapment efficiency (EE) of curcumin within the zein NPs was quantified by separating free (unentrapped) curcumin from the nanoparticle-encapsulated drug via centrifugation (2000 × g, 10 min, 25 °C). The supernatant, containing the curcumin-loaded NPs, was collected, while the pellet (free curcumin) was redissolved in 2 mL of 70 % ethanol. The concentration of free curcumin was determined using a UV-Vis spectrophotometer at 425 nm.[31] A calibration curve (1–10 µg/mL in 70 % ethanol) was established to quantify the drug content (**Fig. S1**, Supplementary Information). The EE was calculated using **eq. 1**.

$$EE\ (\%) = \frac{Curcumin_{total} - Curcumin_{free}}{Curcumin_{total}} \times 100 \qquad (1)$$

View Article Online
DOI: 10.1039/D5TB02868J

Furthermore, the nanoparticles dispersion was freeze-dried. A known quantity of dried nanoparticles was dissolved in 70% ethanol and curcumin concentration was quantified after appropriate dilution. Drug loading (DL) was measured using **eq. 2**.

$$DL\ (\mu g.100mg^{-1}) = \frac{Concentraion\ of\ drug\ (\mu g)}{Amount\ of\ NP\ taken_{\ in\ mg total}} \times 100 \quad (\mathbf{2})$$

2.4. Preparation of gel-precursor solutions

Poloxamer 407 ISFG precursor solution (20% w/w) was prepared by dissolving P407 in distilled water by manual mixing using a spatula for 10 min on an ice bath to prevent premature gelation. The solution was then stored at 4 °C overnight for complete dissolution and bubble removal. For the PEO-poloxamer blend system, poloxamer 407 (18 % w/w) was first dissolved, followed by the addition of PEO (2 % w/w, final) under continuous stirring in an ice bath.

For drug-loaded formulations, metronidazole (MTD, 5 mg/g) was dissolved in water before incorporation into either the 20 % poloxamer or the 18 % poloxamer / 2 % PEO blend. Curcumin-loaded nanoparticles were used to dissolved polymers (20 % or 18 % w/w P407 with 2 % PEO) under ice-cooled stirring to prevent aggregation. In dual-drug formulations, MTD was first dissolved in the NP suspension before adding poloxamer. Details about the composition of precursor solutions of ISGFs are given in **Table 1**.

Table 1 Composition of formulations (in g for 1 g of solution)

Formulation code	P	P+PEO	P-MTD	P+PEO-MTD	P-CZXX or Z50	P+PEO-CZXX or Z50	P-MTD+CZ50	P+PEO-MTD+CZ50
Poloxamer	0.2	0.18	0.2	0.18	0.2	0.18	0.2	0.18
PEO		0.02		0.02		0.02		0.02
Water	0.8	0.8						
Water with MTD (5 mg/g)			0.8	0.8				
CZ50/CZ75/CZ100 or Z50 NP suspension					0.8	0.8		
CZ50 NP suspension with MTD (5 mg/g)							0.8	0.8

2.5. Formulation Characterization

2.5.1. Gelation time and temperature

The gelation time was measured by placing precursor solutions in a water bath from 4 °C to 37 °C. Briefly, precursor solutions (1 g) were added to 5 mL glass vials. They were then placed in a refrigerator (4 °C) for 1 h. Vials were removed and incubated at 37 °C (water bath). After 5 s, gelation was evaluated by inverting vials. For gelation time, vials were incubated in a water bath (Julabo F 25, Germany) at 18 °C. The temperature was increased 0.5 °C every 5 minutes and gelation was observed.[32] The temperature at which gelation occurred was noted as the gelation temperature. Each formulation was tested for three independent samples.

2.5.2. Gel Strength Analysis

The mechanical properties of the hydrogels were evaluated using a Texture Analyzer (TA. XT Plus, Stable Micro Systems Ltd, UK) using a 5-mm cylindrical probe. Hydrogel precursor solutions (5 g) were placed at 37 °C for 30 min to induce gelation before testing. The probe compressed the gel at 2 mm/s to a depth of 10 mm, and the resistance force (gel strength) was recorded. Adhesiveness and cohesiveness were also measured by measuring the negative area and ratio of positive areas of two compressions, respectively (**Fig. S2**, Supplementary information), following a previous study.[33]

2.5.3. Syringeability testing

The ease of administration was assessed by measuring the force required to extrude cold pre-hydrogel solution through a 27G needle. The test was performed at a speed of 1 mm/s, and the extrusion force was recorded using a Texture Analyzer (TA.XT Plus, Stable Micro Systems Ltd., UK) (**Fig. S3**, Supplementary Information). The maximum force (N) required to inject the solution was compared for different formulations. The term "syringeability force" was used in this manuscript.

2.5.4. *In vitro* degradation

The degradation of ISFGs was evaluated using the gravimetric method.[34] Precursor solutions (about 0.5 g) were added to already weighed 15 mL tubes (w_o) and weighed again (w_g). After gelation at 37 °C for 15 minutes, 10 mL of phosphate buffer (pH 6.8) was added, and the tubes were placed in an incubator at 37 °C with shaking at 100 rpm. After 1, 2, 4, 6, 24, and 48 h, the medium was removed from the tubes, and their walls were carefully cleaned using blotting paper, and the tubes were weighed (w_t). The degradation of gels (%) was determined using **eq. 3.**

$$Degradation\ (\%) = \frac{w_t - w_o}{w_g - w_o} \times 100 \quad (\mathbf{3})$$

2.6. *In Vitro* Drug Release Studies

A phosphate buffer (pH 6.8, simulating saliva) was used as the release medium, as reported previously.[35] Hydrogel samples (1 g) were placed in 50 mL Falcon tubes, pre-incubated at 37 °C for 30 min to allow gelation, and then 25 mL of release was added gently onto the gel following shaking at 100 rpm. At predetermined intervals (1, 2, 4, 6, 24, and 48 h), 2 mL aliquots were withdrawn and replaced with fresh buffer. For curcumin release, 1 % w/v Tween 80 was added to the dissolution medium.[36] The released curcumin and MTD were quantified by

View Article Online
DOI: 10.1039/D5TB02682J

measuring absorbance after appropriate dilution at 425 nm and 320 nm using calibration curves, respectively (**Fig. S4**, Supplementary information). Drug release data were fitted for Higuchi and Korsmeyer-Peppas kinetic models using DDsolver, which was also used to calculate the similarity factor for comparisons.[37] Korsmeyer-Peppas model was fit for the initial 6 h as it best fit for 60 % release.[38]

2.7. Antioxidant Activity (DPPH Radical Scavenging Assay)

The antioxidant capacity of curcumin-loaded hydrogels (P-CZ50 and P+PEO-CZ50) was assessed using a DPPH radical scavenging assay. A 12.5 mM DPPH solution was prepared in absolute ethanol for the experiments. Hydrogel samples (0.2 g) were dissolved in 2 mL of deionized water under continuous stirring for 30 minutes to achieve a final concentration of 0.1 g/mL. Aliquots (25, 50, and 100 µL) of these solutions were then mixed with 100 µL of DPPH solution, along with appropriate volumes of water and absolute ethanol to maintain consistent reaction conditions. The mixtures were protected from light and incubated at room temperature for 15 minutes to allow the radical scavenging reaction to occur.

The reaction progress was monitored spectrophotometrically at 517 nm using SPARK® M10 multimode microplate reader (Tecan Trading AG, Switzerland), measuring the characteristic decrease in violet DPPH coloration as an indicator of antioxidant activity. Ascorbic acid (15 µg/mL) served as the positive control for comparison. Blank samples were also prepared with the same volume of ethanol without DPPH and the absorbance of the blank was subtracted from the absorbance of the corresponding sample. The DPPH scavenging activity (%) was calculated using **eq. 4**.

$$DPPH\ scavenging\ avtivity\ (\%) = \left(\frac{A_{Control} - A_{Sample}}{A_{control}}\right) x\ 100 \quad (4)$$

2.8. Stability Study

Formulations stored at 4 °C for 2 months were re-evaluated for Physical stability, gel strength, syringeability force, and drug release (Refer to sections 2.5 and 2.6). The 2-month time point was chosen to illustrate the proof-of-concept that the addition of PEO does not cause immediate physical destabilization (loss of gelation ability and strength) within this very short period.

2.9. Cytocompatibility Assessment

Hydrogel extracts without drugs were prepared by incubating hydrogels for 24 h at 37 °C in full medium. Human dermal fibroblasts (HDFs) were cultured in DMEM supplemented with 10 % FBS and seeded at a density of 20,000 cells/well in 96-well plates. After 24 hours of incubation, the cells were treated with hydrogel extracts (10 and 25 mg/mL) for an additional 24 h. Cell viability was then assessed using the MTT assay, where cells were incubated with MTT reagent (0.5 mg/mL) for 3 h, followed by dissolution of the resulting formazan crystals in DMSO and measurement of absorbance at 590 nm. Relative cell viability was calculated using **eq. 5**. Additionally, a live/dead assay was performed by staining cells with fluorescein diacetate (FDA, 8 µg/mL, green fluorescence for live cells) and propidium iodide (PI, 10 µg/mL, red fluorescence for dead cells) for 5 min. The images were captured using an IncuCyte S3 microscope at 20x magnification. Absolute cell viability was calculated by counting the number of living and dead cells from captured images using **eq. 6**. 20 % DMSO was used as a positive control for cytotoxicity evaluation. Furthermore, cell morphology was also analyzed after staining of paraformaldehyde-fixed cells with Alexa Fluor™ 488 Phalloidin and DAPI.

$$\text{Relative cell viability} = \frac{Absorbance\ of\ test\ well}{Absorbance\ of\ control} \times 100 \quad (5)$$

$$\text{Absolute cell viability} = \frac{Live\ cells\ (Green)}{Total\ cells\ (Green + Red)} \times 100 \quad (6)$$

2.10. Antibacterial Activity

The *in vitro* antibacterial efficacy of the formulations was evaluated against *Porphyromonas gingivalis* (W50 strain) using the agar well diffusion method. Chocolate agar plates (obtained from Universitetstannklinikken, Tromsø, Norway) and hydrogels were pre-warmed to 37 °C for 15 min. A 50 µL aliquot of the bacterial stock was uniformly spread on each plate using an L-shaped disposable spreader, and wells (5.4 mm diameter) were punched into the agar with a sterilized cork borer. Each well was filled with 50 µL of the respective hydrogel formulation using a syringe. Plates were sealed and incubated anaerobically at 37 °C for 48 h in an anaerobic jar containing an AnaeroGen™ 2.5 L sachet and a moist paper to maintain humidity. Following incubation, zones of inhibition (clear areas indicating bacterial growth suppression) were measured. Diameters were determined at three points using a vernier caliper, and the average value was calculated for each formulation. P-MTD, P-MTD+CZ50, and P+PEO-MTD+CZ50 were evaluated for antibacterial activities. Antibacterial activities were also evaluated using the bacterial suspension. For this, 3 mL of bacterial suspension in Tryptic Soy Broth medium with 5% fetal bovine serum on 0.5 g of ISFGs in 15 mL tubes. Tubes with loose caps were then placed in anaerobic jar containing an AnaeroGen™ 2.5 L sachet at 37 °C for 48 h. Optical densities of the suspensions were measured at 600 nm and subtracted from the blank (tube with only medium). Furthermore, 24 h extracts of ISFG (1 g/4 mL of dissolution medium) were also tested. 5 µL of extracts was added to filter paper discs and placed on agar placed. After 48 h of incubation under anaerobic conditions, zones of inhibition were measured.

2.11. Anti-inflammatory activity

Anti-inflammatory activities of extracts CZNP-loaded hydrogels (25 mg/mL) were evaluated using LPS-activated RAW 264.7 macrophages. RAW 264.7 macrophages were cultured in complete DMEM (with 10% FBS, penicillin/streptomycin). For IL-6 quantification 10,000 cells/well were seeded, while 30,000 cells/well were seeded for nitric oxide quantification in a 96-well plate. After 24 hours, the cells were treated for another 24 hours under the following conditions in serum-free medium: (1) negative control (medium only), (2) positive control (1 µg/mL LPS only), and (3) test group (1 µg/mL LPS + 25 mg/mL extract of hydrogels). The anti-inflammatory response was determined by measuring the levels of nitric oxide and IL-6 in the collected supernatants. Nitric oxide was quantified with the Griess assay[39], and IL-6 was measured with a mouse IL-6 ELISA kit (ThermoFisher Scientific, Catalog No. 88–7064). P, P+PEO, P-CZ50, and P+PEO-CZ50 were evaluated for anti-inflammatory activity.

View Article Online
DOI: 10.1039/D5TB02868J

2.12. Statistical Analysis

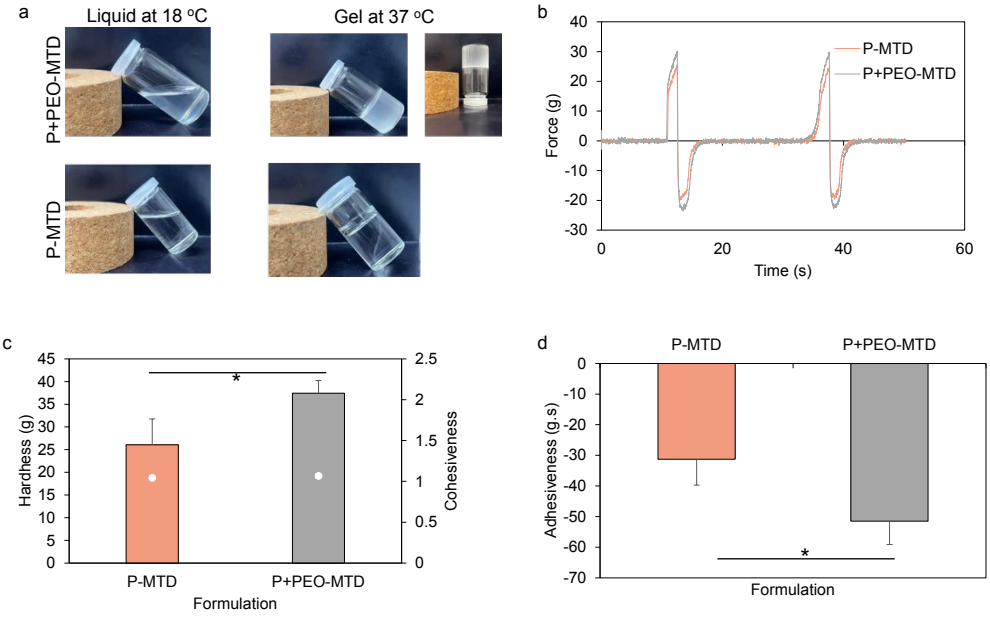

Fig. 1. Characterization of MTD-loaded ISFG systems. (a) Pictures of ISFG systems at 20 °C and 37 °C illustrating thermal gelation. (b) Force-time curves for ISFG systems after forming gels at 2 mm/s probe speed. (c) Hardness (in bars) and cohesiveness (in scatter plot) of gels. (d) Adhesiveness of the gels. * $p < 0.05$

Data are expressed as mean ± standard deviation (SD) (n = 3). Statistical significance was determined using Student's t-test or one-way ANOVA with Tukey's post-hoc test ($p < 0.05$ considered significant).

3. Results and discussion

3.1. Poloxamer-PEO ISFG for water-soluble drug delivery

Poloxamer 407 and PEO are both water-soluble; therefore, a water-soluble drug (MTD) was directly added to prepare precursor solutions of ISFG. It was found that both systems with and without PEO formed hydrogel at 37 °C (**Fig. 1a**), which is important for providing a localized drug delivery. The gelation time and temperature were also determined, and significantly lower gelation times and temperatures were observed with the addition of PEO, while no effect of the drug was observed (**Fig. S5,** Supplementary Information). The mechanical properties of MTD-ISFG systems with and without PEO were compared. The addition of PEO significantly increased ($p < 0.05$) the hardness of the gels from 26.07±5.68 g (P-MTD) to 37.43±1.06 g (P+PEO-MTD) (**Fig. 1b & c**). Cohesiveness was also evaluated, which was about 1 for both formulations, indicating their ability to regain strength after one compression (**Fig. 1c**). Adhesiveness, measured by calculating negative work done required for the probe to retract, was also increased with PEO from -31.27±8.48 g.s for P-MTD to -51.51±7.60 g.s for P+PEO-MTD (Fig. 1d). Overall, gel hardness and adhesiveness were increased with the addition of PEO in MTD-loaded ISFG systems.

An increase in mechanical strength may also affect the syringeability force of the systems, a crucial parameter in determining clinical potential, particularly for periodontal applications. Therefore, syringeability was evaluated through 27 G needle. The addition of PEO caused a significant increase in syringeability force from 10.12±0.91 N (P-MTD) to 15.50±0.66

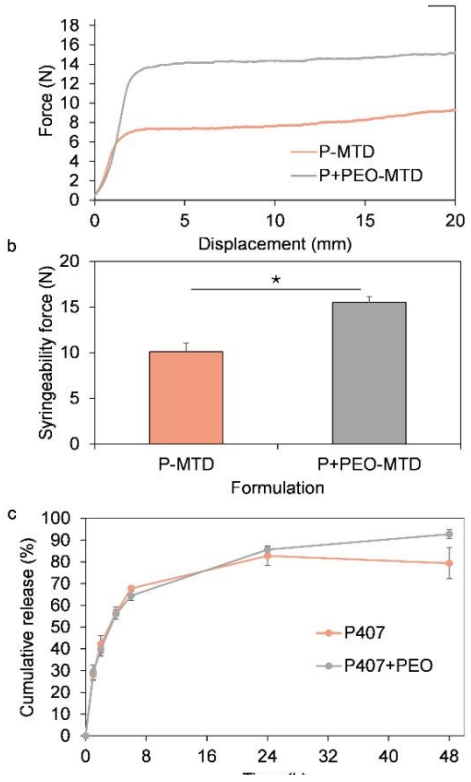

Fig. 2. Syringeability and drug release from MTD-loaded ISFG systems. (a) Force-displacement curves for syringeability through 27G needle. (b) Maximum syringeability force. (c) Cumulative metronidazole release from ISFG systems. * $p < 0.05$

View Article Online
DOI: 10.1039/D5TB02868J

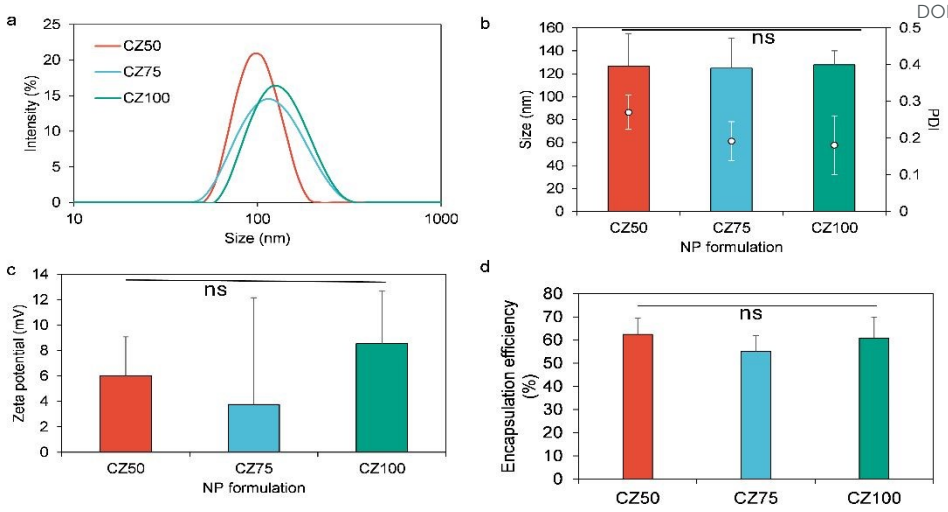

Fig. 3. Characterization of curcumin-loaded zein nanoparticles. (a) Representative size distribution curves for CZ50, CZ75, and CZ100. (b) Mean sizes (bars) and polydispersity indices (PDI)(scatter plot) of CZ50, CZ75, and CZ100. (c) Mean zeta potentials, and (d) Encapsulation efficiency for curcumin. ns – non-significant

N (P+PEO-MTD) (**Fig. 2**). This increase in syringeability force was due to the high viscosity of PEO. However, this force was below the acceptable limit (<40 N).[40] The addition of PEO and increase in strength did not influence the drug release, as similar MTD release profiles ($f_2 > 50$) were observed from ISFG systems with and without PEO (**Fig. 2**). The degradation rates of the ISFG systems were also evaluated, and the results showed that PEO can decrease the degradation rate (**Fig. S6**, Supplementary Information), which shows that degradation was not the key mechanism for drug release.

For water-insoluble or hydrophobic drug delivery, curcumin was selected. It has antioxidant and anti-inflammatory activities that are especially beneficial for the treatment of periodontitis.[21]

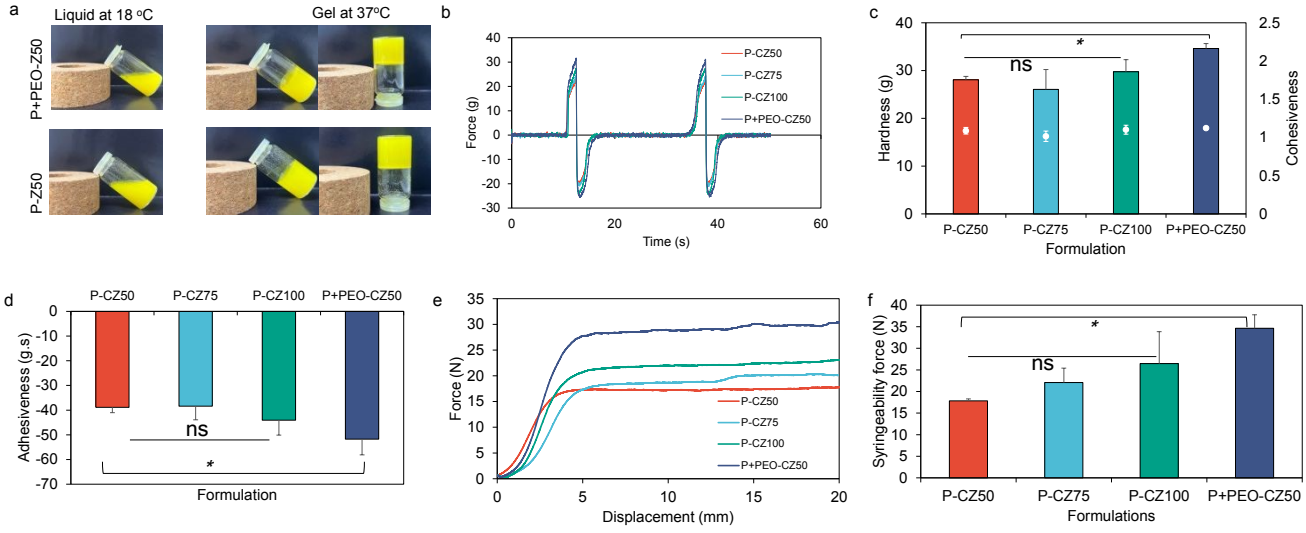

Fig. 4. Characterization of CZ-loaded ISFG systems. (a) Pictures of Z50-loaded ISFG systems at 20 °C and 37 °C illustrating thermal gelation. (b) Force-time curves for CZNP-loaded ISFG systems after forming gels at 2 mm/s probe speed. (c) Hardness and cohesiveness of gels. (d) Adhesiveness of the gels. (e) Force-displacement curves for syringeability through 27G needle. (f) Maximum syringeability force. * $p < 0.05$, ns – non-significant (analysis was performed by one-way ANOVA for P-CZ50, P-CZ75, and P-CZ100; and Students t-test for P-CZ50 and P+PEO-CZ50)

3.2. Poloxamer-PEO ISFG for water-insoluble drug delivery

Direct incorporation of curcumin into ISFG systems was not feasible due to the precipitation of curcumin in poloxamer 407.[16] Therefore, zein nanoparticles were formulated with three different zein concentrations. Three nanoparticle formulations exhibited no significant difference in hydrodynamic size, zeta potential, and encapsulation efficiency (**Fig. 3a-d**). Mean PDI was decreased with an increase in zein concentration from 0.269±0.046 (CZ50) to 0.180±0.080 (CZ100); however, no significant difference ($p > 0.05$) was observed (**Fig. 3b**). Zeta potential was about neutral (> ±10 mV)[41] and encapsulation

View Article Online
DOI: 10.1039/D5TB02868J

efficiency was greater than 50 % for three formulations (**Fig. 3c & d**). Overall, zein concentration (50 - 100 mg) for preparing nanoparticles did not affect size, zeta potential, PDI, and encapsulation efficiency. However, drug loading was decreased with an increase in zein concentration because of the same curcumin concentration for the three formulations (**Fig. S7,** Supplementary Information).

ISFG systems were prepared with CZ50, CZ75, and CZ100 with and without PEO. The effect of PEO was similar to that of MTD-loaded hydrogels, i.e., PEO caused an increase in gel strength, adhesiveness, reduction in gelation time, temperature, and degradation rates (**Fig. 4a and Fig. S8 & S9,** Supplementary Information). Considering the effect of nanoparticles, no significant difference was observed in strength and adhesiveness for P-CZ50, P-CZ75, and P-CZ100 (**Fig. 4b & c**). Syringeability force of these formulations increased from 17.83±0.45 N (for P-CZ50) to 26.46±7.57 N (for P-CZ100); however, no significant difference ($p > 0.05$) was observed (**Fig. 4d & e**). The syringeability force of P+PEO-CZ50 was 34.64±3.12 N, which was significantly higher ($p < 0.05$) than P-CZ50 (17.83±0.45 N), but still lower than the acceptable limit (40 N) (**Fig. 4d & e**). Comparing metronidazole-loaded ISFG systems with NP-loaded ISFG systems, NP-loaded ISFG systems exhibited a higher syringeability force that was due to the resistance of flow caused by nanoparticles through the needle (**Fig. 2 and Fig. 4**).

For the drug release of curcumin, Tween 80 was added to the dissolution medium to increase the solubility of curcumin. A similar behavior of drug release was observed for all three formulations prepared only with P407 i.e., faster release in the beginning and slower after 6 h (**Fig. 5a**). However, the addition of PEO influenced drug release (**Fig. 5b**). In the beginning, the release was slower for the formulation with PEO, while higher release was observed after 16 h. It is relevant to mention here that we did not find a significant difference in MTD release with

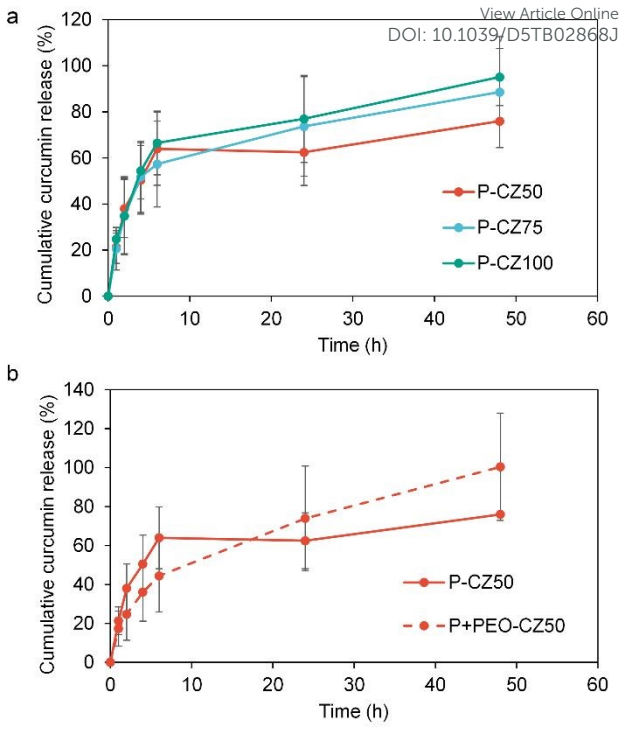

Fig. 5. Release of curcumin from ISFG systems. (a) Cumulative curcumin release from ISFG systems with different nanoparticle formulations. (b) Cumulative curcumin release from CZ50-loaded ISFG systems with and without PEO to evaluate the effect of PEO on curcumin release.

the addition of PEO to ISFG. Therefore, the difference in release for curcumin suggested that PEO may affect nanoparticles with the hydrophobic drug, causing a slower initial release. We proposed that PEO may form a coating around nanoparticles that might restrict the release in the beginning. To validate this, we added the PEO solution to the nanoparticles dispersion and found a significant increase in size (**Fig. S10**, Supplementary

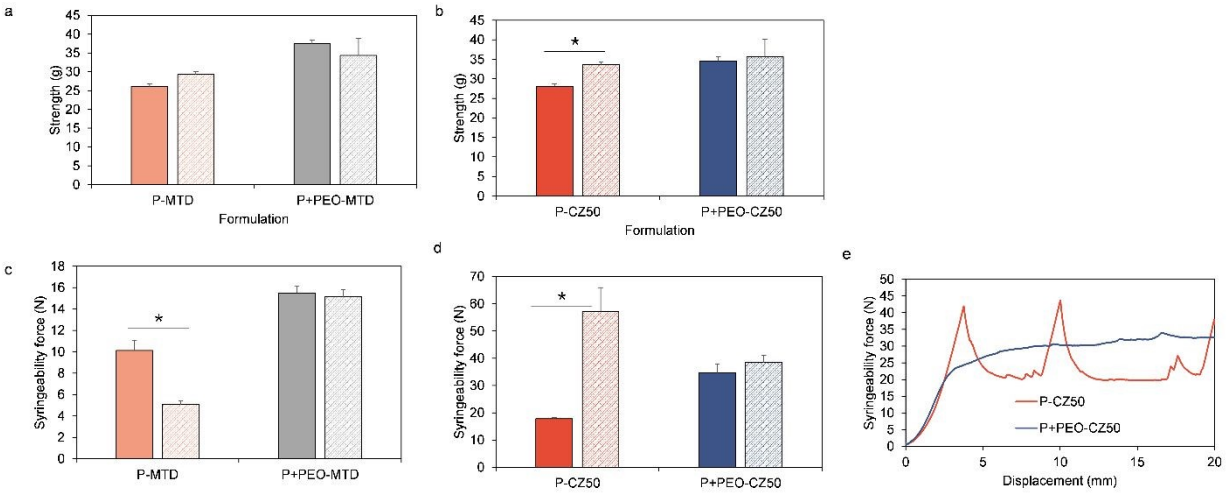

Fig. 6. Effect on gel strength and syringeability force during stability study. Strength of fresh (filled bars) and after 2 months at 4 °C (a) for P-MTD and P+PEO-MTD and (b) for P-Z50 and P+PEO-Z50. Maximum syringeability forces of fresh (filled bars) and after storage for 2 months at 4 °C (c) for P-MTD and P+PEO-MTD and (d) for P-Z50 and P+PEO-Z50. (e) Force-displacement curves for syringeability through 27G needle after storage for 2 months at 4 °C for P-Z50 and P+PEO-Z50, indicating fluctuations for P-Z50. * $p < 0.05$

View Article Online
DOI: 10.1039/D5TB02868J

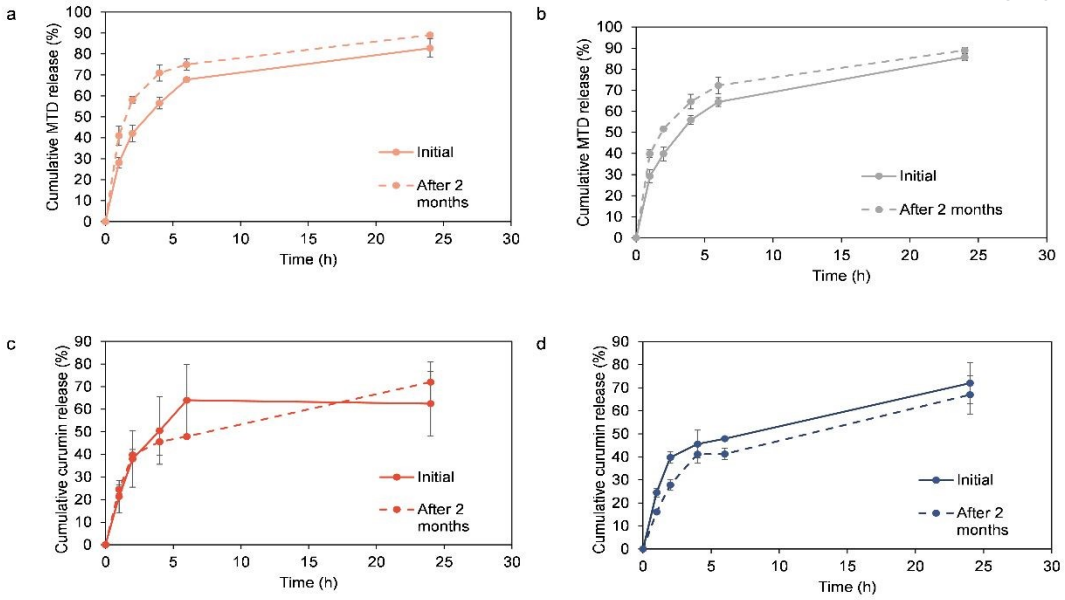

Fig. 7. Effect on drug release during stability study. MTD release from freshly prepared (initial) and stored ISFG for 2 months at 4 °C (a) for P-MTD and (b) P+PEO-MTD. Curcumin release from ISFG systems for fresh and after storage for 2 months at 4 °C (c) for P-CZ50 and (d) P+PEO-CZ50.

Information); however, no increase in size was observed with the addition of an equivalent concentration of P407. Furthermore, the release data were fitted to the Higuchi and Korsmeyer-Peppas kinetic models. P+PEO-CZ50 formulations showed a good fit for Higuchi model with R^2 = 0.959, while P-CZ50 exhibited a poor fit with an R^2 = 0.444, indicating diffusion-controlled release in P+PEO-CZ50. The release exponent "n" in the Korsmeyer-Peppas model was 0.584 for P-CZ50 and 0.549 for P+PEO-CZ50, indicating anomalous transport for both formulations. Overall, it was found that initial release in both formulations was governed by diffusion and swelling/polymer relaxation (as indicated by the release exponent n > 0.45) but diffusion was the leading mechanism for P+PEO-CZ50 (fitting Higuchi Model) (**Table S1**, Supplementary Information).

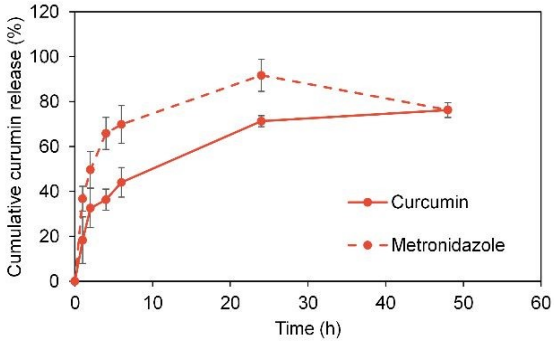

Fig. 8. Cumulative metronidazole and curcumin release from dual drug-loaded ISFG.

3.3. Stability study

Another important property is the stability of the formulation, which was evaluated at 4 °C due to the thermosensitive nature of poloxamer. Gel strength, injectability, and drug release profiles were assessed for stability parameters to determine the effect of PEO on formulation stability. Gel strengths were found to be stable over a 2-month storage period, as no significant difference was observed for all ISFG systems with and without PEO (**Fig. 6a & b**). However, storage affected syringeability force to a greater extent. For P-MTD, a significant reduction ($p < 0.05$) in syringeability force was observed (**Fig. 6c**). However, no significant change was observed with P+PEO-MTD (**Fig. 6c**). Interestingly, formulation with zein nanoparticles (P-Z50) exhibited significantly higher injectability (>40 N, acceptable limit), while P+PEO-CZ50 demonstrated no significant change and injectability fell within acceptable limit (**Fig. 6d**). When force displacement curves were compared for P-CZ50 and P+PEO-CZ50, it was found that the nonuniform flow of P-CZ50 through the needle was responsible for the higher injectability force as shown in irregular force curves in **Fig. 6e**. This nonuniform force was probably due to the strong aggregation of nanoparticles that obstructed the uniform flow of the ISFG system, leading to fluctuating higher syringeability force. On the other hand, PEO may prevent strong aggregation of particles so they can be extruded during the syringeability test under continuous force. It can be inferred that PEO can enhance the stability of the nanoparticles in the ISFG system, preventing strong aggregation during storage.

3.4. Co-delivery of hydrophilic and hydrophobic drugs

View Article Online
DOI: 10.1039/D5TB02681

MTD and curcumin-loaded ISFG systems were evaluated for different parameters individually and found that the incorporation of nanoparticles increased the syringeability force. We also prepared a formulation with both MTD (hydrophilic) and curcumin (hydrophobic). Drug release profiles from co-delivery systems were the same as those of the individual ISFG system (**Fig. 8**). Metronidazole was released faster than curcumin due to the incorporation of curcumin in nanoparticles. Overall, the prepared ISFG system was effective for the co-delivery of hydrophilic and hydrophobic drugs.

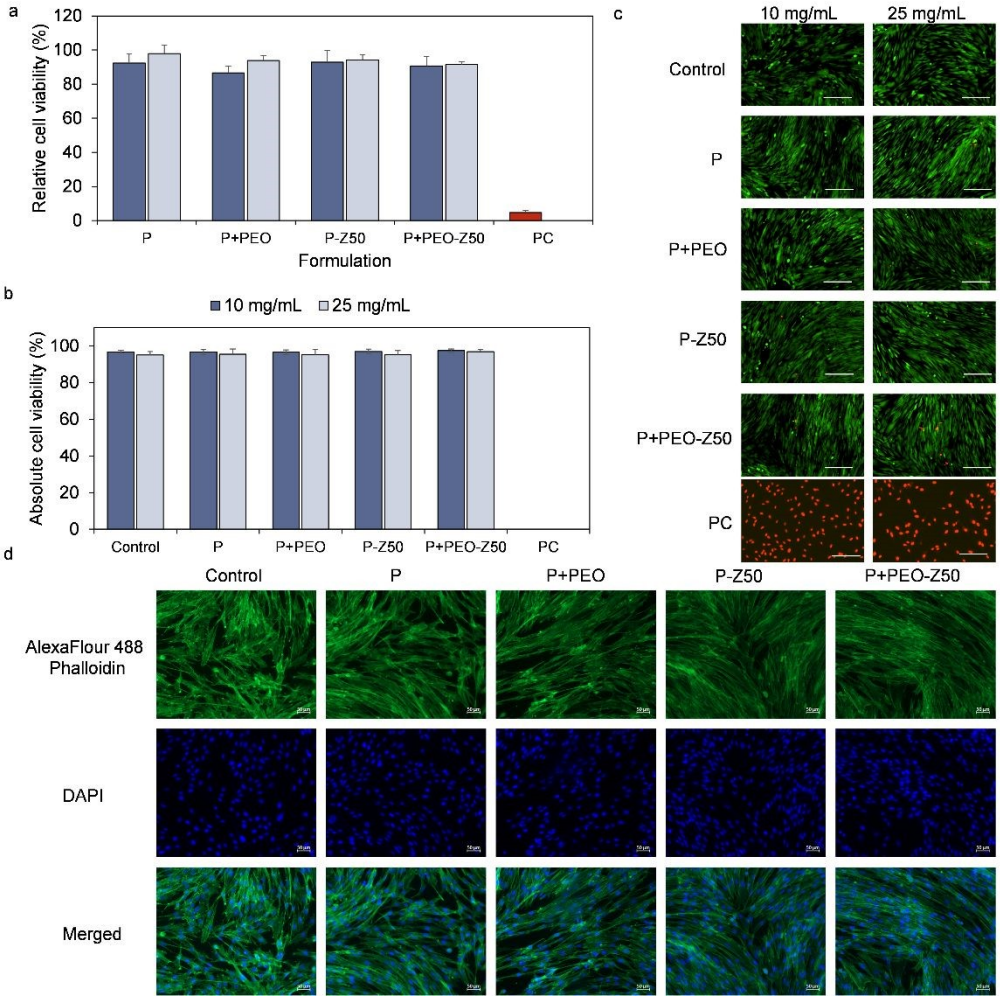

Fig. 9. *In vitro* cytocompatibility of ISFG systems. (a) Relative cell viabilities of HDF cells after treating with 10 and 25 mg/mL extracts of ISFG systems. (b) Absolute cell viabilities of HDF cells after treating with 10 and 25 mg/mL extracts of ISFG systems. (c) Representative images of cells after staining with FDA/PI (PC – positive control, scale bar – 200 µm). (d) Images of cells after staining with AlexaFlour™ 488 and DAPI to evaluate morphologies of cells.

3.5. *In vitro* cytocompatibility

Cytocompatibility is also an important parameter for evaluating drug delivery systems. ISFG systems with and without PEO were evaluated for cytocompatibility of the vehicle (without drugs) as curcumin has GRAS status by the FDA and MTD is already used in clinical practice at higher doses (400 mg).[42, 43] It was found that the 24 h-extracts of ISFG systems at 25 mg/mL were cytocompatible with relative cell viability greater than 80 % (**Fig. 9a**). Absolute cell viability was also evaluated by live/dead staining and found to be greater than 90 % (**Fig. 9b & c, Fig. S11-S12,** Supplementary Information). All systems with and without nanoparticles and PEO were found cytocompatible and no significant difference was observed after the addition of nanoparticles and PEO to poloxamer 407. Poloxamer 407 and zein are biocompatible materials and have a generally recognized as safe (GRAS) status by the FDA.[44, 45] Cells were also stained with DAPI and AlexaFluor™ 488 Phalloidin to stain nuclei and cytoskeleton, respectively. Treatments with hydrogel extracts did not affect the morphologies of cells as given in **Fig. 9d**. Overall, the ISFG systems exhibited no cytotoxicity up to tested concentration, which was primarily due to the selection of biocompatible materials. At higher doses (1.7-5.0 g/kg i.p.), poloxamer 407 may cause renal toxicity that should be considered while administering,[46] depending on the application for which the system is going to be used. For periodontal application, approximately 0.2 mL injection volume is required, which is lower (40 mg of P407/inj.) than the toxicity level considering normal saliva production (0.3-1.5 mL/min).[47]

3.6. *In vitro* antibacterial activity

View Article Online
DOI: 10.1039/D5TB02681

Antibacterial activity of ISFG systems was also assessed, considering their potential application in periodontitis. Porphyromonas gingivalis was used for the evaluation, which is a common cause of periodontitis. Metronidazole is effective against P. gingivalis with a minimum inhibitory concentration of 2 µg/mL.[48] P+PEO-MTD, P-MTD+CZ50, and P+PEO-MTD+CZ50 exhibited clear zone of inhibitions (**Fig. 10a & b**), indicating their antibacterial efficacy. Zone of inhibition of P+PEO-MTD was

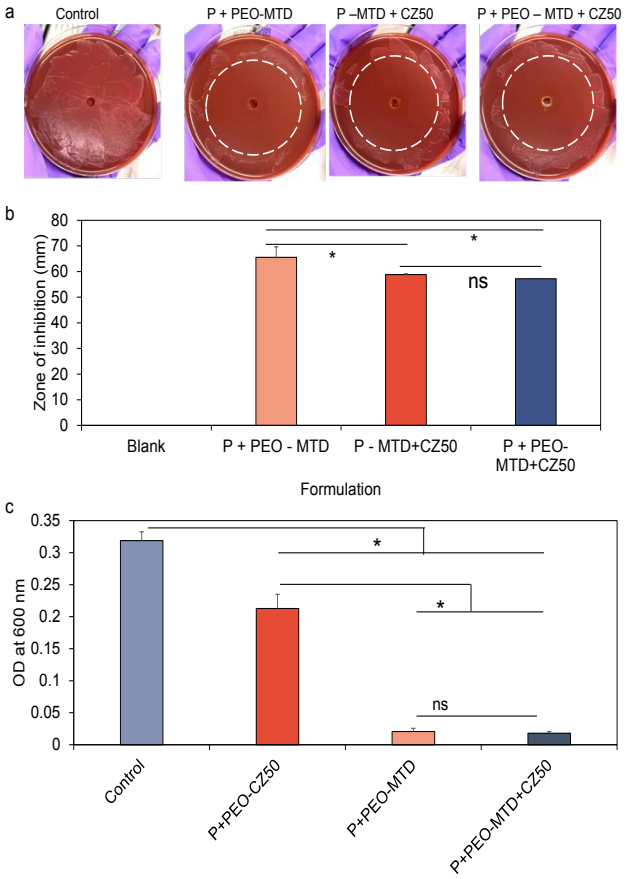

Fig. 10. Antibacterial activity of ISFG systems. (a) Pictures of plates for control and ISFGs treated *P. gingivalis* and (b) corresponding mean zones of inhibition. (c) Optical densities of bacterial suspensions after incubation with different ISFG. * $p < 0.05$

65.56±1.04 mm that was significantly higher ($p < 0.05$) than P-MTD+CZ50 (58.82±4.07 mm) and P+PEO-MTD+CZ50 (57.21±0.28 mm). The addition of PEO did not influence the antibacterial activity, as P-MTD+CZ50 and P+PEO-MTD+CZ50 showed no significant difference ($p > 0.05$). However, curcumin-loaded zein nanoparticles demonstrated a reduced zone of inhibition. We expected that curcumin could increase the antibacterial activity by synergizing with metronidazole, but the results were contradictory. Curcumin was reported to have antibacterial activity against anaerobic bacteria, including *P. gingivalis*.[49] However, in the present work, no synergistic effect with metronidazole was found; instead, it reduced the zone of inhibition. Therefore, liquid broth was also used to evaluate the antibacterial activity of ISFG, and the optical density of broth treated with P+PEO-CZ50 was significantly reduced compared to the control, but remained higher compared to P+PEO-MTD and P+PEO-MTD+CZ50 (**Fig. 10c**). There was no significant difference observed between P+PEO-MTD and P+PEO-MTD+CZ50, which showed that CZ50 did not affect the antibacterial activity of MTD as demonstrated in the agar diffusion assay. We proposed that the use of nanoparticles in the agar diffusion method may lead to insufficient diffusion of insoluble curcumin, causing no effect on curcumin.[50] Moreover, nanoparticles, by binding to agar in a well, may also resist the diffusion of metronidazole in the agar, resulting in a smaller zone of inhibition for P-MTD+CZ50 and P+PEO-MTD+CZ50. Therefore, we also evaluated the antibacterial activity of extracts of P+PEO-MTD and P+PEO-MTD+CZ50 that showed no significant difference in zone of inhibition (**Fig. S13**, Supplementary Information), validating the impact of nanoparticles on metronidazole diffusion in agar.

3.7. *In vitro* antioxidant and anti-inflammatory activity

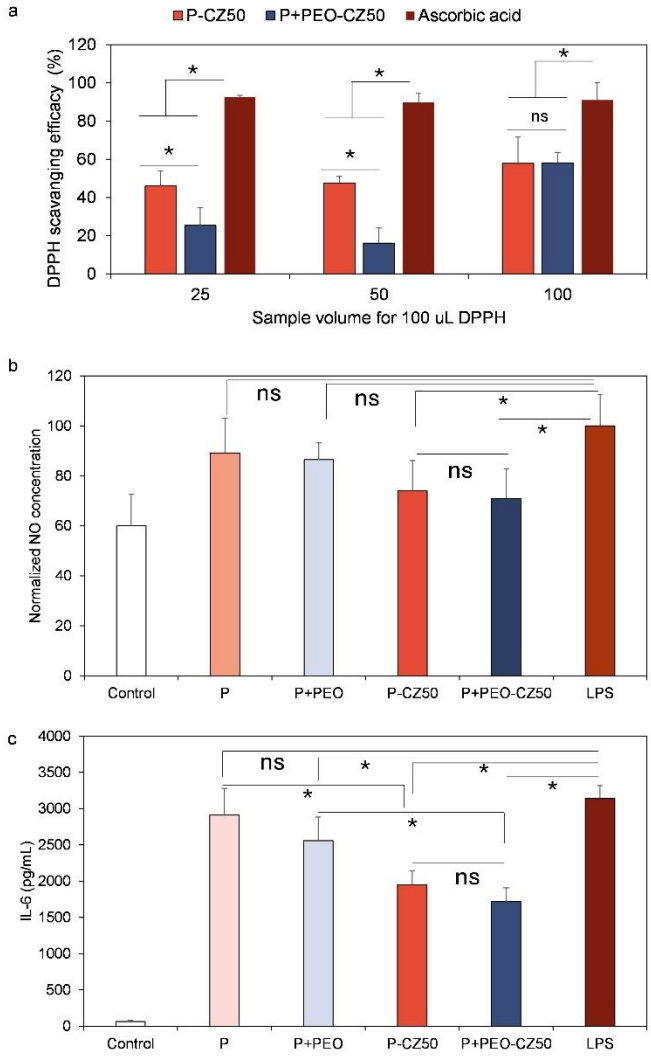

Fig. 11. Antioxidant and anti-inflammatory activities of CZ50-loaded ISFG system. (a) DPPH scavenging efficacy using different volumes of hydrogel extracts (0.1 g/mL). (b) Nitric oxide concentration in cell medium of RAW 264.7 cells after LPS +/- hydrogel extract (25 mg/mL) treatments (Normalized data, LPS = 100 %). (c) IL-6 concentration in cell medium of RAW 264.7 cells after LPS +/- hydrogel extract (25 mg/mL) treatments.* $p < 0.05$

In addition to bacterial infection, the accumulation of reactive oxygen species and pro-inflammatory factors is also involved in

View Article Online
DOI: 10.1039/D5TB02868J

periodontal disease, complicating recovery.[51] Therefore, the antioxidant and anti-inflammatory activities of ISFG systems may impart beneficial effects in treating periodontitis. Curcumin is well known for its antioxidant and anti-inflammatory activity. [21] Therefore, the addition of curcumin in the ISFG systems is crucial for a positive impact in the treatment. P-CZ50 and P+PEO-CZ50 were evaluated for antioxidant activity using DPPH assay. Both exhibited DPPH scavenging efficacy >50% for 100 µL of 0.1 g/mL of ISFG system's extract (**Fig. 11a**). For 25 and 50 µL P-CZ50 exhibited higher efficacy in DPPH scavenging than P+PEO-CZ50; however, no difference was observed at 100 µL (**Fig. 11a**).

Anti-inflammatory activity of curcumin-loaded formulations i.e. P-CZ50 and P+PEO-CZ50 was also evaluated in lipopolysaccharide (LPS)-treated macrophages. It was found that nitric oxide and IL-6 were significantly reduced with treatment of P-CZ50 and P+PEO-CZ50 extracts in LPS-induced activation of macrophages (**Fig. 11b & c**). Overall, curcumin could provide local antioxidant and anti-inflammatory activities in the periodontal cavity environment, establishing a favorable environment for gum recovery.

4. Conclusion

Overall, this study successfully developed and characterized a promising PEO-enhanced poloxamer 407 *in situ* forming gel system for the localized co-delivery of antibacterial and anti-inflammatory agents in periodontitis treatment. The primary challenge of improving the mechanical robustness of P407 gels was effectively overcome by the addition of PEO, which significantly increased gel strength and adhesiveness without compromising injectability. The formulations, whether loaded with hydrophilic metronidazole or hydrophobic curcumin via nanoparticles, exhibited sustained release, antibacterial activity, antioxidant activity, anti-inflammatory activity, and cytocompatibility. A key finding was the superior stabilizing effect of the PEO-P407 matrix on curcumin-loaded zein nanoparticles, preventing aggregation and maintaining syringeability upon storage, an issue observed in the system without PEO. These results collectively emphasize the dual role of PEO in not only reinforcing the mechanical properties of thermosensitive gels but also in ensuring the physical stability of encapsulated nanoparticulate systems. Therefore, the PEO-P407 platform presents a promising and versatile strategy for advanced, localized drug delivery in the management of complex periodontal disease. Although the present study was focused on periodontal disease, we propose that the addition of PEO to P407-based thermosensitive formulations may also benefit other localized drug delivery applications via dual drug delivery. A comprehensive *in vitro* evaluation of the prepared formulations was performed; however, the absence of *in vivo* validation in an animal model and a prolonged stability study are limitations that will be addressed in future work. Furthermore, the syringeability force increased with the incorporation and became closer to the acceptable limit that should be considered while optimizing formulation in the future.

Author contributions

Ali Raza: conceptualization, methodology, investigation, formal analysis and writing – original draft. Piarina Reginold: investigation, and writing – original draft. Nataša Škalko-Basnet: Project administration and writing – review and editing. Sybil Obuobi: conceptualization, project administration, funding acquisition, supervision, and writing – review and editing.

Conflicts of interest

There are no conflicts to declare.

Data availability

The data supporting the findings of this study can be obtained from the corresponding author upon reasonable request. The data supporting this article have been included as part of the supplementary information (SI). Supplementary information (SI) is available online.

Acknowledgements

This work was supported by Tromsø Research Foundation (TFS) through the TFS starting grant (20_SG_SO) to Dr. Obuobi. We thank Dr. Tracy Munthali Lunde for providing *P. gingivalis*. We thank the Department of Pharmacy, UIT The Arctic University of Norway, for providing research support.

References

1. G. E. M. Villoria, R. G. Fischer, E. M. B. Tinoco, J. Meyle and B. G. Loos, *Periodontol 2000*, 2024, **96**, 7-19.
2. C. M. Ardila and J. A. Bedoya-Garcia, *J Glob Antimicrob Resist*, 2020, **22**, 215-218.
3. F. Graziani, D. Karapetsa, B. Alonso and D. Herrera, *Periodontol 2000*, 2017, **75**, 152-188.
4. M. Amato, S. Santonocito, A. Polizzi, G. M. Tartaglia, V. Ronsivalle, G. Viglianisi, C. Grippaudo and G. Isola, *Pharmaceutics*, 2023, **15**, 1312.
5. R. Ashfaq, B. Sisa, A. Kovacs, S. Berko, M. Szecsenyi, K. Burian, P. Valyi and M. Budai-Szucs, *Eur J Pharm Sci*, 2023, **191**, 106607.
6. F. Batool, K. Agossa, M. Lizambard, C. Petit, I. M. Bugueno, E. Delcourt-Debruyne, N. Benkirane-Jessel, H. Tenenbaum, J. Siepmann, F. Siepmann and O. Huck, *Int J Pharm*, 2019, **569**, 118564.
7. M. P. Do, C. Neut, H. Metz, E. Delcourt, K. Mader, J. Siepmann and F. Siepmann, *Int J Pharm*, 2015, **486**, 38-51.
8. A. Raza, U. Hayat, X. Zhang and J. Y. Wang, *Int J Pharm*, 2022, **627**, 122206.
9. R. R. Thakur, H. L. McMillan and D. S. Jones, *J Control Release*, 2014, **176**, 8-23.

10. A. Garg, R. Agrawal, C. Singh Chauhan and R. Deshmukh, *Int J Pharm*, 2024, **652**, 123819.
11. P. Chomchalao, N. Saelim, S. Lamlertthon, P. Sisopa and W. Tiyaboonchai, *J Drug Deliv Sci Tec*, 2024, **99**, 105988.
12. P. Zheng, X. Liu, Y. Jiao, X. Mao, Z. Zong, Q. Jia, H. B. Jiang, E. S. Lee and Q. Chen, *Tissue Eng Regen Med*, 2024, **21**, 1153-1171.
13. H. Zhou, M. Yuan and T. Zhang, *Journal*, 2025, **17**, 451.
14. R. Ashfaq, A. Kovacs, S. Berko and M. Budai-Szucs, *Biomed Pharmacother*, 2025, **183**, 117836.
15. H. Abdeltawab, D. Svirskis and M. Sharma, *Expert Opin Drug Deliv*, 2020, **17**, 495-509.
16. A. D. Jose, K. L. Foo, G. Hu, L. Ngar, B. Ryda, J. Jaiswal, Z. Wu, P. Agarwal and S. S. Thakur, *Eur J Pharm Biopharm*, 2024, **201**, 114372.
17. M. A. Serbanescu, M. Oveisi, C. Sun, N. Fine, A. Bosy and M. Glogauer, *Front Oral Health*, 2022, **3**, 933997.
18. N. Lopez-Valverde, A. Lopez-Valverde, J. Montero, C. Rodriguez, B. Macedo de Sousa and J. M. Aragoneses, *Front Bioeng Biotechnol*, 2023, **11**, 1226907.
19. N. T. Hashim, R. Babiker, M. M. Rahman, R. Mohamed, S. P. Priya, N. C. Chaitanya, M. S. Islam and B. Gobara, *Molecules*, 2024, **29**.
20. P. L. Ravishankar, Y. P. Kumar, E. N. Anila, P. Chakraborty, M. Malakar and R. Mahalakshmi, *Int J Pharm Investig*, 2017, **7**, 188-192.
21. S. M. Solomon, C. S. Stafie, I. G. Sufaru, S. Teslaru, C. M. Ghiciuc, F. D. Petrariu and O. Tanculescu, *Pharmaceutics*, 2022, **14(5)**, 982.
22. T. Ur-Rehman, S. Tavelin and G. Grobner, *Int J Pharm*, 2011, **409**, 19-29.
23. M. Dewan, G. Sarkar, M. Bhowmik, B. Das, A. K. Chattoapadhyay, D. Rana and D. Chattopadhyay, *Int J Biol Macromol*, 2017, **102**, 258-265.
24. W. Boonlai, V. Tantishaiyakul, N. Hirun, T. Sangfai and K. Suknuntha, *Aaps Pharmscitech*, 2018, **19**, 2103-2117.
25. H. R. Lin, K. C. Sung and W. J. Vong, *Biomacromolecules*, 2004, **5**, 2358-2365.
26. K. M. Ranch, F. A. Maulvi, A. R. Koli, D. T. Desai, R. K. Parikh and D. O. Shah, *Aaps Pharmscitech*, 2021, **22**, 77.
27. S. Kawasaki and M. Kobayashi, *Colloids and Surfaces A: Physicochemical and Engineering Aspects*, 2018, **537**, 236-242.
28. X. Li and K. Hyun, *Korea-Aust Rheol J*, 2018, **30**, 109-125.
29. J. Cs, M. Haider, M. Rawas-Qalaji and P. Sanpui, *Colloids Surf B Biointerfaces*, 2025, **245**, 114319.
30. S. Podaralla and O. Perumal, *Aaps Pharmscitech*, 2012, **13**, 919-927.
31. Q. Gu, G. Lu, J. Han, D. J. McClements, C. Ma, X. Liu and F. Liu, *Int J Biol Macromol*, 2025, **309**, 142884.
32. J. C. Gilbert, J. L. Richardson, M. C. Davies, K. J. Palin and J. Hadgraft, *J Control Release*, 1987, **5**, 113-118.
33. J. B. da Silva, M. T. Cook and M. L. Bruschi, *Carbohydr Polym*, 2020, **240**, 116268.
34. P. X. Zheng, X. Y. Liu, Y. Q. Jiao, X. R. Mao, Z. R. Zong, Q. Jia, H. B. Jiang, E. S. Lee and Q. Chen, *Tissue Eng Regen Med*, 2024, **21**, 1153-1171.
35. M. R. C. Marques, R. Loebenberg and M. Almukainzi, *Dissolut Technol*, 2011, **18**, 15-28.
36. K. Shahani and J. Panyam, *J Pharm Sci*, 2011, **100**, 2599-2609.
37. Y. Zhang, M. R. Huo, J. P. Zhou, A. F. Zou, W. Z. Li, C. L. Yao and S. F. Xie, *Aaps J*, 2010, **12**, 263-271.
38. N. A. Peppas and J. J. Sahlin, *Int J Pharmaceut*, 1989, **57**, 169-172.
39. L. C. Green, D. A. Wagner, J. Glogowski, P. L. Skipper, J. S. Wishnok and S. R. Tannenbaum, *Anal Biochem*, 1982, **126**, 131-138.
40. R. P. Watt, H. Khatri and A. R. G. Dibble, *Int J Pharm*, 2019, **554**, 376-386.
41. J. D. Clogston and A. K. Patri, *Methods Mol Biol*, 2011, **697**, 63-70.
42. P. Eickholz, R. Koch, M. Göde, K. Nickles, T. Kocher, K. Lorenz, T. S. Kim, J. Meyle, D. Kaner, U. Schlagenhauf, I. Harks and B. Ehmke, *J Clin Periodontol*, 2023, **50**, 1239-1252.
43. J. Z. Song, Y. L. Liu, L. F. Lin, Y. Zhao, X. Q. Wang, M. Zhong, T. G. Xie, Y. T. Luo, S. J. Li, R. C. Yang and H. Li, *Rsc Adv*, 2019, **9**, 40131-40145.
44. C. Minnelli, P. Moretti, G. Fulgenzi, P. Mariani, E. Laudadio, T. Armeni, R. Galeazzi and G. Mobbili, *Int J Pharm*, 2018, **552**, 225-234.
45. R. Paliwal and S. Palakurthi, *J Control Release*, 2014, **189**, 108-122.
46. G. Dumortier, J. L. Grossiord, F. Agnely and J. C. Chaumeil, *Pharm Res*, 2006, **23**, 2709-2728.
47. A. M. Pedersen, A. Bardow, S. B. Jensen and B. Nauntofte, *Oral Dis*, 2002, **8**, 117-129.
48. T. Larsen, *Oral Microbiol Immunol*, 2002, **17**, 267-271.
49. A. M. Sha and B. T. Garib, *Biomed Res Int*, 2019, **2019**, 6810936.
50. A. Kourmouli, M. Valenti, E. van Rijn, H. J. E. Beaumont, O. I. Kalantzi, A. Schmidt-Ott and G. Biskos, *J Nanopart Res*, 2018, **20**.
51. M. Martinez-Garcia and E. Hernandez-Lemus, *Front Physiol*, 2021, **12**, 709438.

View Article Online
DOI: 10.1039/D5TB02868J

The data supporting this article have been included as part of the Supplementary Information. Supplementary information: Figures S1, S2, S4, S5, S6, Calibration curves, confocal images and further experimental details. See DOI: [URL – format https://doi.org/DOI]